

## Stable $[\text{Pb}(\text{ROH})_N]^{2+}$ Complexes in the Gas Phase: Softening the Base To Match the Lewis Acid

Glen Akibo-Betts, Perdita E. Barran, Ljiljana Puskar, Bridgette Duncombe, Hazel Cox, and Anthony J. Stace\*

*Contribution from the School of Chemistry, Physics, and Environmental Sciences, University of Sussex, Falmer, Brighton, BN1 9QJ, U.K.*

Received December 14, 2001

**Abstract:** Experiments have been performed in the gas phase to investigate the stability of complexes of the general form  $[\text{Pb}(\text{ROH})_N]^{2+}$ . With water as a solvent, there is no evidence of  $[\text{Pb}(\text{H}_2\text{O})_N]^{2+}$ ; instead  $[\text{PbOH}(\text{H}_2\text{O})_{N-1}]^+$  is observed, where lead is considered to be held formally in a +2 oxidation state by the formation of a hydroxide core. As the polarizability of the solvating ligands is increased through the use of straight chain alcohols, ROH, solvation of  $\text{Pb}^{2+}$  is observed without proton transfer when  $R \geq \text{CH}_3\text{CH}_2\text{-CH}_2\text{-}$ . The relative stabilities of  $[\text{Pb}(\text{ROH})_4]^{2+}$  complexes with respect to proton transfer are further investigated through the application of density functional theory to examples where  $R = \text{H}$ , methyl, ethyl, and 1-propyl. Of three trial structures examined for  $[\text{Pb}(\text{ROH})_4]^{2+}$  complexes, in all cases those with the lowest energy comprised of three solvent molecules were directly bound to the central cation, with the fourth molecule held in a secondary shell by hydrogen bonds. The implications of this arrangement as a favorable starting structure for proton transfer are discussed. Conditions for the stability of particular Pb(II)/ligand combinations are also discussed in terms of the hard–soft acid–base principle. Charge population densities calculated for the central lead cation and oxygen donor atoms across the ROH range are used to support the proposal that proton transfer occurs when a ligand is hard. Stability of the  $[\text{Pb}(\text{ROH})_4]^{2+}$  unit is commensurate with a decrease in the ionic character of the bond between  $\text{Pb}^{2+}$  and a ligand; this in turn reflects a softening of the ligand as the alkyl chain increases in length. From the calculations, the most favorable protonated product is, in all cases,  $(\text{ROH})_2\text{H}^+$ . The trends observed with lead are compared with Cu(II), which is capable of forming stable gas-phase complexes with water and all of the alcohols considered here.

### Introduction

The body of work based around metal ion chemistry in the gas phase has increased enormously in the past 15 years, ranging from early work examining the solvation and reactions of singly charged ions<sup>1–5</sup> to studies of metal ions in high oxidation states in conjunction with biologically relevant molecules.<sup>6–8</sup> Findings from both experimental and theoretical studies of metal ions are employed increasingly to facilitate explanations of behavior in solution-phase chemistry and biological systems.<sup>9,10</sup> In condensed-phase chemistry, several different factors are recognized as contributing to the stability of complexes containing

monodentate ligands  $[\text{M}(\text{L})_N]^{z+}$ . A commonly used qualitative assessment is the hard–soft acid–base (HSAB) principle as outlined by Pearson.<sup>11</sup> This simple model assumes that in a bond between any two atoms, one will play the part of an acid and the other a base. In essence, HSAB postulates that highly charged small cations of low polarizability (hard acids) will form strong bonds with ligands of low polarizability (hard bases) and weak bonds with soft bases (high polarizability), and vice versa for soft acids (high polarizability). While often criticized as semiquantitative, as it ignores interactions between the complex and the bulk solvent (for example, counterion hydration energies), it can be usefully employed to explain results from gas-phase measurements of complex formation.<sup>12,13</sup> Kearble and Deng have obtained free energy changes for the reaction  $\text{ML}_2^+ = \text{M}^+ + 2\text{L}$  for  $\text{M} = \text{Cu}^+$ ,  $\text{Ag}^+$ , and  $\text{Li}^+$  with several different ligands and report partial confirmation of the HSAB principle in that stronger bonds (as shown by more negative  $\Delta H$  values) are formed with  $\text{Cu}^+$  and  $\text{Ag}^+$  (termed soft acids) by soft ligands than with  $\text{Li}^+$  (a hard acid) by the same ligands. However, Kearble and Deng warn that other interactions, such

\* To whom correspondence should be addressed. E-mail: tonys@sussex.ac.uk.

- (1) Eller, K.; Schwartz, H. *Chem Rev.* **1991**, *91*, 1121.
- (2) Kearble, P. *Annu. Rev. Phys. Chem.* **1977**, *28*, 445.
- (3) Huang, S.; Holman, R. W.; Gross, M. L. *Organometallics* **1986**, *5*, 1857.
- (4) Jacobsen, D. B.; Freiser, B. S. *J. Am. Chem. Soc.* **1985**, *107*, 67.
- (5) Keese, R. G.; Castleman, A. W., Jr. *J. Phys. Chem. Ref. Data* **1986**, *15*, 1011.
- (6) Nemirovsky, O. V.; Gross, M. L. *J. Am. Soc. Mass Spectrom.* **1998**, *9*, 1285.
- (7) Lavanant, H.; Hecquet, E.; Hoppilliard, Y. *Int. J. Mass Spectrom.* **1999**, *185/186/187*, 11.
- (8) Grese, R. P.; Cerny, R. L.; Gross, M. L. *J. Am. Chem. Soc.* **1989**, *111*, 2835.
- (9) Blades, A. T.; Jayaweera, P.; Ikonou, M. G.; Kebarle, P. *J. Chem. Phys.* **1990**, *92*, 5900.
- (10) Dudev, T.; Cowan, J. A.; Lim, C. *J. Am. Chem. Soc.* **1999**, *121*, 7665.

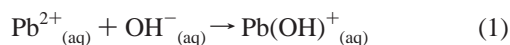
- (11) Pearson, R. G. *J. Chem. Educ.* **1968**, *45*, 581, 643.
- (12) Deng, H.; Kerbarle, P. *J. Am. Chem. Soc.* **1998**, *120*, 2825.
- (13) Deng, H.; Kerbarle, P. *J. Phys. Chem. A* **1999**, *103*, 11246.

as multipole forces, which are not formally included in the HSAB principle may also affect bond energies.<sup>12,13</sup>

Contreras and co-workers have made an analysis of proton transfer in the gas-phase acid–base equilibria of alkyl-substituted alcohols.<sup>14</sup> This theoretical study uses an ion transport model to quantify the charge redistribution associated with proton transfer and essentially supports the experimental work of Brauman and Blair<sup>15</sup> by asserting that the acidity of alcohols in the gas phase increases as a function of the length of the alkyl chain. This finding may be rationalized in terms of HSAB because a proton is the hardest possible acid, and as increased alkyl substitution occurs the corresponding alkoxide ion becomes a softer base; hence the O–H bond weakens.

This laboratory has recently developed an efficient gas-phase technique for generating multiply charged metal ions solvated by a wide variety of oxygen and nitrogen donating ligands. The approach has begun to contribute to an analysis of the interactions responsible for the stability and coordination of a central metal ion (M) in association with *N* ligands (L), in the form of a gas-phase complex with the general description  $[M(L)_N]^{2+}$ . Thus far, the experiments have provided a qualitative picture of solvation for the metal ions Cu(II),<sup>16,17</sup> Ag(II),<sup>17,18</sup> Au(II),<sup>17,19</sup> Mg(II),<sup>20</sup> and Mn(II).<sup>21</sup>

In keeping with our observations on gold(II) and silver(II),<sup>17–19</sup> lead(II) does not yield stable complexes of the form  $[M(H_2O)_N]^{2+}$ . For gold(II), there is no evidence that  $[Au(H_2O)_N]^{2+}$  ions exist in the liquid phase, and for silver(II),  $[Ag(H_2O)_N]^{2+}$  ions are only stable under acidic conditions strong enough to counteract the oxidizing nature of the metal ion.<sup>22</sup> In the case of lead(II), measurements have been made of the acidity constant ( $pK_a$ ) for the reaction:<sup>23</sup>



Relevant to this study are data from Pedersen et al.<sup>24</sup> (taken at “approaching” zero ionic strength) where a  $pK_a$  of 7.8 has been determined. In the context of gas-phase experiments on  $[M(H_2O)_N]^{2+}$  ions, it is interesting to note that stable Cu(II) complexes can be formed with water,<sup>25</sup> even though the  $pK_a$  value for this ion is reported to be  $\sim 7.5$ . Given the similarity in  $pK_a$  values for Pb(II) and Cu(II), this contrast in behavior is unexpected; however, it is quite possible that differences in the way the two ions coordinate water molecules (see below) may contribute to the ease of formation of the hydrolysis product on the part of Pb(II). Related to these issues is the observation of many groups of polynuclear hydroxocations,  $M_q(OH)_p^{(nq-p)+}$ , which result from hydrolysis reactions and in the case of lead,

for example, yield ions of the form  $Pb_2(OH)^{3+}$ ,  $Pb_4(OH)_4^{4+}$ , and  $Pb_6(OH)_8^{4+}$ .<sup>26,27</sup> Multiple proton loss in aqueous systems normally requires high pH values; however, the conditions under which polynuclear cations are observed for Cu(II) are markedly different from those which favor their formation with Pb(II). On the basis of mobility measurements in aqueous solution, various estimates place the hydration number for  $Pb^{2+}$  between 4 and 7.5.<sup>28</sup>

In recent years, improvements in the speed and accuracy of computational methods have led to theory being increasingly employed to substantiate experimental observations on multiply charged metal ion complexes.<sup>29</sup> Such studies may also provide insight into why a given metal–ligand combination is unstable or even unobservable as an ion in the gas phase. With respect to the coordination chemistry of lead, Bock and co-workers<sup>30</sup> have recently analyzed crystallographic data on di- and tetravalent compounds. Supported by ab initio molecular orbital calculations, they have sought to establish what influence the electron lone pair on Pb(II) has on the binding and orientation of ligands. The lack of participation in bonding of this so-called “inert pair” has been attributed to relativistic effects.<sup>31</sup> Bock and co-workers<sup>30</sup> find that for Pb(II) complexes with coordination numbers between 2 and 5, the ligands adopt a hemi-directed arrangement (as opposed to being evenly distributed) about the central metal ion; in other words, lone pair–ligand repulsion prevails over ligand–ligand repulsion.

In this paper, results are presented of a gas-phase study of the solvation of Pb(II) with water and a series of straight chain alcohols as ligands. An attempt is made to interpret the data in terms of established gas-phase acid–base behavior on the part of the alcohols studied.<sup>14</sup> The application of density functional theory provides relative stabilization energies for  $[Pb(ROH)_4]^{2+}$  complexes with respect to proton-transfer products in the form of  $[PbOR(ROH)_{2-x}]^+ + ROH_2^+ \cdot (ROH)_x$ . These calculations help to explain the absence of  $[Pb(ROH)_N]^{2+}$  complexes when R = H, methyl, or ethyl, and their presence when R = propyl or butyl. The variation in charge population on the central metal cation and on the donor oxygen atoms within each complex examined supports the premise of a HSAB approach, which relies on a decrease in basicity of the solvating alcohols as the alkyl chain length increases.

## Experimental Section

The experimental setup has been described in detail elsewhere.<sup>32</sup> Lead pellets (Sigma-Aldrich) in an effusive source (DCA Instruments) held at between 900 and 950 °C yield  $\sim 10^{-2}$  mbar of lead vapor. This region is crossed with a beam of neutral mixed solvent–argon clusters, which are formed by the adiabatic expansion of a ROH/argon mixture through a pulsed supersonic nozzle. The solvents used were water, methanol, ethanol, propan-1-ol, and butan-1-ol. All alcohols were obtained from Sigma-Aldrich and were of spectroscopic purity. The clusters pass through a 1 mm diameter skimmer into the path of the

(14) Perez, P.; Toro-Labbe, A.; Contreras, R. *J. Phys. Chem. A* **1999**, *103*, 11246.

(15) Brauman, J. I.; Blair, L. K. *J. Am. Chem. Soc.* **1970**, *92*, 5986.

(16) Wright, R. R.; Walker, N. R.; Firth, S.; Stace, A. J. *J. Phys. Chem. A* **2001**, *105*, 54.

(17) Walker, N. R.; Wright, R. R.; Barran, P. E.; Murrell, J. N.; Stace, A. J. *J. Am. Chem. Soc.* **2001**, *123*, 4223.

(18) Walker, N. R.; Wright, R. R.; Stace, A. J. *J. Am. Chem. Soc.* **1999**, *121*, 4837.

(19) Walker, N. R.; Wright, R. R.; Barran, P. E.; Stace, A. J. *Organometallics* **1999**, *18*, 3569.

(20) Walker, N.; Dobson, M. P.; Wright, R. R.; Barran, P. E.; Murrell, J. N.; Stace, A. J. *J. Am. Chem. Soc.* **2000**, *122*, 11138.

(21) Cox, H.; Walker, N. R.; Wright, R. R.; Stace, A. J., in preparation.

(22) Cotton, F. A.; Wilkinson, G. *Advanced Inorganic Chemistry*; Wiley: London, 1988.

(23) (a) Pokriš, B.; Putar, Z. *J. Inorg. Nucl. Chem.* **1973**, *35*, 1987. (b) Hugel, R. *Bull. Soc. Chim. Fr.* **1964**, 1462. (c) Hugel, R. *Bull. Soc. Chim. Fr.* **1965**, 968.

(24) Pedersen, K. J. K. *Dan. Vidensk. Selsk., Mat.-Fys. Medd.* **1945**, *22*, 29.

(25) Stace, A. J.; Walker, N. R.; Firth, S. *J. Am. Chem. Soc.* **1997**, *119*, 10239.

(26) Burgess, J. *Metal Ions in Solution*; Wiley: London, 1978.

(27) Baes, C. F.; Mesmer, R. E. *The Hydrolysis of Cations*; Wiley: New York, 1976.

(28) Conway, B. E. *Ionic Hydration in Chemistry and Biophysics*; Elsevier: Amsterdam, 1981.

(29) Katz, A. K.; Glusker, J. P.; Beebe, S. A.; Bock, C. W. *J. Am. Chem. Soc.* **1996**, *118*, 5752.

(30) Shimoni-Livny, L.; Glusker, J. P.; Bock, C. W. *Inorg. Chem.* **1998**, *37*, 1853.

(31) Pyykkö, P. *Chem. Rev.* **1988**, *88*, 563.

(32) Woodward, C. A.; Dobson, M. P.; Stace, A. J. *J. Phys. Chem. A* **1997**, *101*, 2279.

metal vapor, where the mixed solvent–argon clusters pick up lead atoms. These neutral clusters then enter the ion source of a high-resolution double-focusing mass spectrometer (VG ZAB-E) where they are ionized by electron impact at 100 eV. In combination with the thermal pick-up process, ionization is thought to cause complete evaporation of the rare gas atoms from the clusters (no ions of the form  $\text{Pb}(\text{L})_N\text{Ar}_M^{2+}$  are detected). Previous experiments have indicated that the presence of rare gas atoms as an energy sink is essential to the pick-up process.<sup>33</sup>

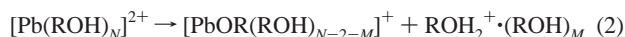
A shutter situated at the top of the oven enables an unambiguous assignment of signals caused by metal-containing species, and values recorded for parent and fragment ion intensities represent differences between shutter open and shut signals. This step is necessary as solvent clusters dominate the cluster beam. Evidence for the formation of a hydroxide core is obtained by examining products arising from collisional activation. For this purpose, the background pressure in a cell situated next to the single focusing slit in the second field free region of the mass spectrometer is increased to approximately  $10^{-6}$  mbar. Reaction products are identified by systematically scanning the voltage of the electrostatic analyzer,<sup>34</sup> a procedure that results in a mass-analyzed ion kinetic energy (MIKE) spectrum.

### Computational Details

The reported calculations were performed using the Amsterdam density functional (ADF) package.<sup>35</sup> The numerical integration procedure applied for the calculations is that of te Velde and Baerends,<sup>36</sup> and energies of the structures were calculated using the local density approximation (LDA) from Vosko et al.<sup>37</sup> The nonlocal exchange of Becke,<sup>38</sup> the nonlocal correlation correction of Perdew,<sup>39</sup> and the scalar relativistic correction<sup>40</sup> were applied to the LDA density.

A double- $\zeta$  Slater-type-orbital (STO) basis set was used to describe the valence electrons of Pb, and hydrogen, oxygen, and carbon were described by double- $\zeta$  STOs augmented with polarization functions. The core atomic orbitals of lead were set as [Hg] and treated by the frozen core approximation. Similarly, the 1s orbitals of carbon and oxygen were also treated as frozen cores. To improve the accuracy of calculated energies, single point energy calculations were performed on optimized geometries using triple- $\zeta$  basis sets, again with hydrogen, carbon, and oxygen characterized by additional polarization functions and with the frozen core of lead reduced to [Xe]. Trial optimizations, using the larger basis set and smaller Pb core, indicated that the ordering of the relative stabilities of optimized structures was not altered.

The calculations focused on the proton-transfer process observed in the experiments, which can be characterized as



where R = H, methyl, ethyl, or propyl. The calculations were performed for  $N = 4$  and all possible values of  $M$ , that is,  $M = 0-2$ . In each case, the energies of all constituents on either side of eq 2 were calculated.

The objective was to establish both an electrostatic and an energetic basis for the observed stabilization of  $\text{Pb}^{2+}$  complexes for  $R \geq$  propyl. As a result of these calculations, a Mulliken charge population analysis (MPA)<sup>41</sup> was derived for the central lead cation and donor oxygen atoms. These data provide a qualitative scale with which to demonstrate the stabilization which afforded divalent lead by water and the series

of alcohols. In addition, the degree of covalency of the lead–alcohol bond is assessed by an analysis of orbital occupancy (6s and 6p) and the extent of sp hybridization.

Although in general terms, all forms of charge population analysis are questionable, MPA is possibly most open to criticism,<sup>42</sup> and yet remains one of the most widely used. To give a more complete picture of the distribution of charge within lead–alcohol complexes, and to provide comparisons with the work of Bock et al.,<sup>30</sup> a natural population analysis (NPA) was also performed. Because ADF does not have a capability for generating NPA output, single point calculations on complexes previously optimized with ADF were conducted using Gaussian 98.<sup>43</sup> The Gaussian 98 calculations were performed at the B3PW91/LANL2DZ computational level. Natural bond orbital (NBO) analysis provided further insight into the distribution of electrons, including occupancy of the lead atom lone pair, and these data aid comparisons between the various Pb(II) complexes. All computational findings are presented in the discussion section where their relevance to the experimental results is assessed.

### Results

Experimental measurements covered the intensities and collision-induced dissociation spectra of singly and doubly charged ions of the form  $[\text{PbOR}(\text{ROH})_N]^+$  and  $[\text{Pb}(\text{ROH})_N]^{2+}$ , respectively. These data are used to assess the stabilization of lead in a +2 oxidation state by ligands for which  $R \leq$  propyl and to explore the competition between hydroxide/alkoxide formation and direct solvation. Individual ligand types are considered in turn.

**I. Pb and Water.** Parent ion intensities recorded for  $[\text{PbOH}(\text{H}_2\text{O})_N]^+$ ,  $[\text{Pb}(\text{H}_2\text{O})_N]^{2+}$ , and  $[\text{Pb}(\text{H}_2\text{O})_N]^+$  are shown in Figure 1a as a function of  $N$  for the range  $N = 1-7$ . No evidence for more than one proton loss was found for any value of  $N$ , but, in each case, peaks corresponding to protonated forms of the ions were present with intensities approximately 5% of those of the unprotonated forms. The contribution to signals recorded for  $[\text{Pb}(\text{H}_2\text{O})_N]^{2+}$ , from ions of the form  $[\text{PbOH}(\text{H}_2\text{O})_{N-1}]^+$ , was assessed on the basis of signals recorded for  $[\text{PbOH}(\text{H}_2\text{O})_{N-1}]^+$  ions and scaled according to the relative isotopic contribution. Ion intensities for  $[\text{Pb}(\text{H}_2\text{O})_N]^+$  complexes containing the 206 and the 208 lead isotopes follow a pattern that is typical for hydrated metal ions in the gas phase, where, after  $N = 2$ , ions have a near exponential decline in intensity. Deviations from this behavior could be indicative of particular structural stability or instability, the former being the so-called “magic numbers”. The behavior of  $[\text{Pb}(\text{H}_2\text{O})_N]^+$  contrasts with the intensities recorded for  $[\text{PbOH}(\text{H}_2\text{O})_N]^+$  ions, where the decline in intensity after  $N = 1$  (corresponding to  $N = 2$  for simple hydrated ions) is more gradual, possibly indicating a higher (relative) stability for these ions as  $N$  increases. If a metal hydroxide core is formed, then the addition of subsequent water ligands could be favored when compared

- (33) Winkel, J. F.; Jones, A. B.; Woodward, C. A.; Kirkwood, D. A.; Stace, A. J. *J. Chem. Phys.* **1994**, *101*, 9436.  
 (34) Cooks, R. G.; Beynon, J. H.; Caprioli, R. M.; Lester, G. R. *Metastable Ions*; Elsevier: Amsterdam, 1973.  
 (35) ADF 2.3.0 Theoretical Chemistry, Vrije Universiteit, Amsterdam.  
 (36) te Velde, G.; Baerends, E. J. *J. Comput. Phys.* **1992**, *99*, 84.  
 (37) Vosko, S. H.; Wilk, L.; Nusair, M. *Can. J. Phys.* **1980**, *58*, 1200.  
 (38) Becke, A. D. *Phys. Rev. A* **1988**, *38*, 3098.  
 (39) Perdew, J. P. *Phys. Rev. B* **1986**, *33*, 8822.  
 (40) Snijders, J. G.; Baerends, E. J. *Mol. Phys.* **1978**, *36*, 1789.  
 (41) Mulliken, R. S. *J. Chem. Phys.* **1962**, *36*, 3428.

- (42) Jensen, F. *Introduction to Computational Chemistry*; John Wiley & Sons: Chichester, 1999.  
 (43) Frisch, M. J.; Trucks, G. W.; Schlegel, H. B.; Scuseria, G. E.; Robb, M. A.; Cheeseman, J. R.; Zakrzewski, V. G.; Montgomery, J. A.; Stratmann, R. E.; Burant, J. C.; Dapprich, S.; Millam, J. M.; Daniels, A. D.; Kudin, K. N.; Strain, M. C.; Farkas, O.; Tomasi, J.; Barone, V.; Cossi, M.; Cammi, R.; Mennucci, B.; Pomelli, C.; Adamo, C.; Clifford, S.; Ochterski, J.; Petersson, G. A.; Ayala, P. Y.; Cui, Q.; Morokuma, K.; Malick, D. K.; Rabuck, A. D.; Raghavachari, K.; Foresman, J. B.; Cioslowski, J.; Ortiz, J. V.; Stefanov, B. B.; Liu, G.; Liashenko, A.; Piskorz, P.; Komaromi, I.; Gomperts, R.; Martin, R. L.; Fox, D. J.; Keith, T.; Al-Laham, M. A.; Peng, C. Y.; Nanayakkara, A.; Gonzalez, C.; Challacombe, M.; Gill, P. M. W.; Johnson, B. G.; Chen, W.; Wong, M. W.; Andres, J. L.; Head-Gordon, M.; Replogle, E. S.; Pople, J. A. *Gaussian 98*, revision A.7; Gaussian, Inc.: Pittsburgh, PA, 1998.

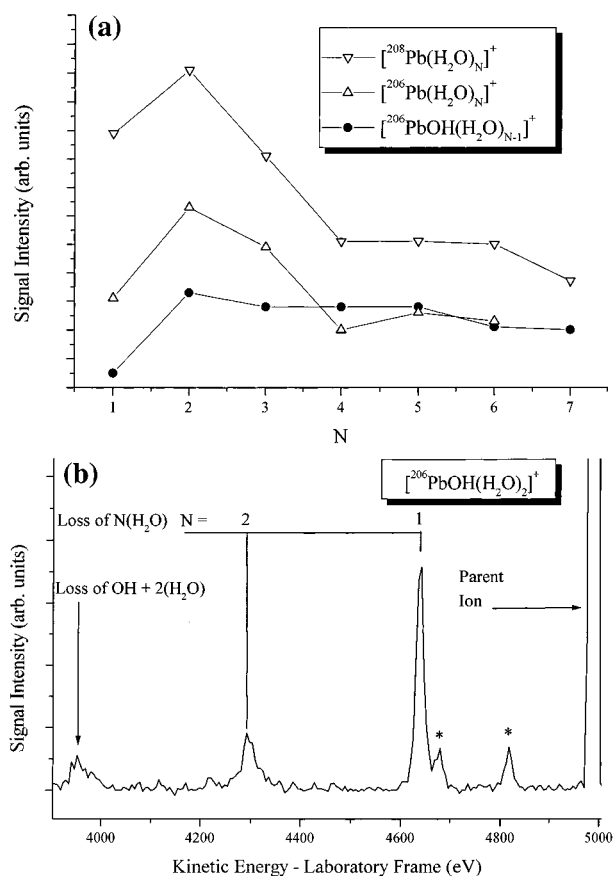


**Figure 1.** (a) Parent ion intensities recorded for singly charged lead/water complexes plotted as a function of size; (b) section of a MIKE scan performed on  $[^{206}\text{PbOH}(\text{H}_2\text{O})_2]^+$  in the presence of air as a collision gas and at a pressure of  $10^{-6}$  mbar. Impurity peaks are indicated by \*.

with  $[\text{Pb}(\text{H}_2\text{O})_N]^+$  complexes, as the nominal positive charge on the lead may be higher. Likewise, increased polarization of first shell molecules will result in stronger hydrogen bonding to molecules in subsequent shells. Similar patterns of behavior are to be seen in the work of Fuke et al.<sup>44</sup> on  $\text{Mg}^+(\text{H}_2\text{O})_N$  and  $\text{Mg}^+\text{OH}(\text{H}_2\text{O})_N$ . For both magnesium and lead, a more realistic description of the hydroxide core would be to assume it adopts the form  $\text{M}^{2+}-\text{OH}^-$ . Such an interpretation is supported by the charge population analysis of solvated lead hydroxides and alkoxides presented below.

Figure 1b presents the results of a MIKE scan of the ion  $[^{206}\text{PbOH}(\text{H}_2\text{O})_2]^+$ . Signals caused by the loss of neutral ligands from the metal ion are annotated, and impurity peaks are labeled (\*). Major peaks after the parent ion correspond to  $[^{206}\text{PbOH}(\text{H}_2\text{O})]^+$  and  $[^{206}\text{PbOH}]^+$  (i.e., the loss of one and two water molecules, respectively), and the final peak is  $^{206}\text{Pb}^+$ , which arises from the loss of two water molecules and the OH group. While a MIKE scan can give no indication as to whether ligand loss is simultaneous or sequential, the implication from Figure 1b is that the OH group is more tightly bound to the metal ion than are the two water ligands. There is no evidence for OH loss unless accompanied by the loss of all solvating water molecules. Similarly, there is no evidence for loss of  $\text{OH}^-$ ; however, this is not too surprising because the energy difference between the electron affinity of OH and the second ionization

energy of lead is large (15.03 eV). MIKE scans performed for  $N = 3$  and 4 also show the loss of the OH group only when accompanied by the loss of  $N$  water molecules. For  $N \geq 5$ , the energy resolution was not sufficient to differentiate between OH and  $\text{H}_2\text{O}$  loss.

**II. Methanol and Ethanol.** For methanol and ethanol, information qualitatively similar to that shown for the lead/water system was obtained, with clusters of the general form  $[\text{Pb}(\text{ROH})_N]^+$  and  $[\text{PbOR}(\text{ROH})_N]^+$  being observed in the mass spectra. There was no evidence for ions of the form  $[\text{Pb}(\text{ROH})_N]^{2+}$  with either alcohol at any value of  $N$ . Plots equivalent to that shown in Figure 1a for methanol and ethanol show that for  $[\text{Pb}(\text{ROH})_N]^+$  clusters the parent ion intensities decrease rapidly from  $N = 1$  for ethanol and slightly less rapidly from  $N = 2$  for methanol. The intensities of the  $[^{206}\text{PbOR}(\text{ROH})_N]^+$  complexes for both alcohols exhibit behavior slightly different from that seen for water, with the ions of maximum intensity appearing at  $N = 3$ . As before, collision-induced dissociation of ions of the general form  $[^{206}\text{PbOR}(\text{ROH})_N]^+$  indicates the presence of a  $[\text{Pb}^{2+}-\text{OR}^-]$  core because there is no evidence for the loss of OR prior to the loss of  $N(\text{ROH})$ .

**III. Propan-1-ol and Butan-1-ol.** In contrast to all of the previous examples, doubly charged  $[\text{Pb}(\text{ROH})_N]^{2+}$  complexes were observed with both of these ligands. For propan-1-ol,  $N$  covers the range 3–10, and for butan-1-ol,  $3 \leq N \leq 6$ . Signals were present at higher values of  $N$  for both ions, but their intensities were too low to justify inclusion. Ions of the form  $[\text{PbOR}(\text{ROH})_N]^+$  and  $[\text{Pb}(\text{ROH})_N]^+$  were also observed in the mass spectra. Figure 2a shows a plot of the relative intensities of the ions  $[\text{PbOR}(\text{ROH})_{N-1}]^+$  and  $[\text{Pb}(\text{ROH})_N]^{2+}$  for R = propyl. The singly charged ions are more abundant, at all values of  $N$ , but, as a function of size, their decrease in intensity is more marked than for the doubly charged ions. For  $[\text{PbOpropyl}(\text{propan-1-ol})_N]^+$  complexes, their intensities decline from  $N = 2$  onward; in contrast, the doubly charged ions exhibit an intensity maximum at  $N = 4$ , which could be indicative of a particularly stable metal/ligand combination. The corresponding data for butan-1-ol exhibit intensity maxima at  $N = 4$  and 5, which again could be evidence of stable structures.

The presence of doubly charged ions is confirmed by mass selecting a given complex and subjecting it to collisional activation, such that the products of charge and/or proton transfer are evident. Figure 2b shows one such example, where the ion  $[^{208}\text{Pb}(\text{propan-1-ol})_6]^{2+}$  has undergone collisional activation in the presence of air. The MIKE scan contains a number of unassigned peaks (labeled \*) caused by the dissociation of an ion that is mass coincident with  $[^{208}\text{Pb}(\text{propan-1-ol})_6]^{2+}$ . These peaks were distinguished by rerunning the CID spectrum over the same energy range, but with the temperature of the effusive cell reduced to a point where lead complexes were no longer observed. Peaks caused by both neutral ligand loss and ligand loss accompanied by charge transfer are present in the MIKE scan. The largest neutral fragmentation peak is caused by the loss of two propan-1-ol molecules from the parent ion to give  $[\text{Pb}(\text{propan-1-ol})_4]^{2+}$ . This observation is consistent with the parent ion intensities in Figure 2a, which show the  $N = 4$  ion as the most intense (stable) ion. Likewise, the absence of any significant  $[\text{Pb}(\text{propan-1-ol})_3]^{2+}$  product would also match the experimental results in Figure 2a.

(44) Misaizu, F.; Sanekata, M.; Iwata, S.; Fuke, K. *J. Chem. Phys.* **1994**, *100*, 2.

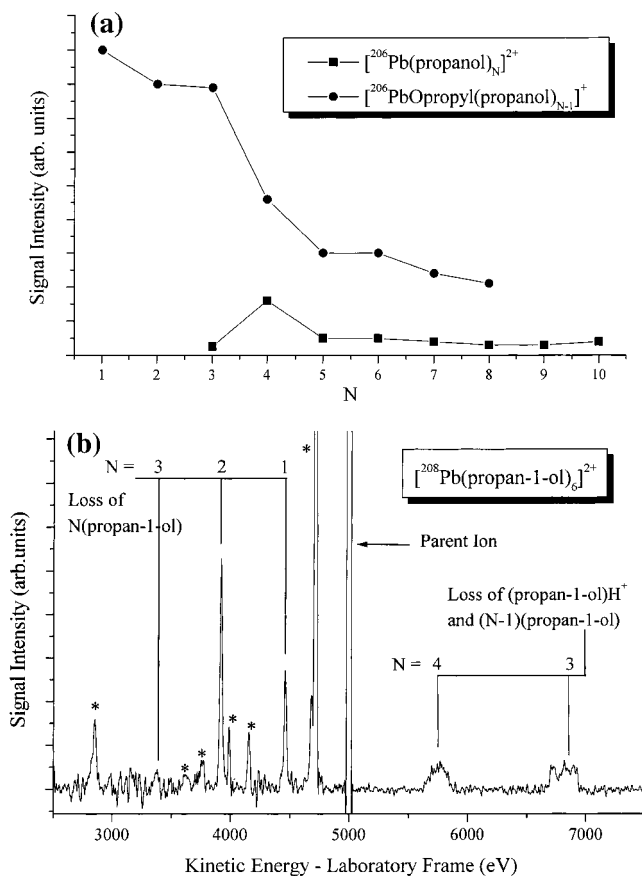


**Figure 2.** (a) Parent ion intensities recorded for the ions  $[\text{Pb}(\text{propan-1-ol})_N]^{2+}$  and  $[\text{PbOpropyl}(\text{propan-1-ol})_{N-1}]^+$  plotted as a function of  $N$ ; (b) MIKE scan performed on  $[\text{Pb}(\text{propan-1-ol})_4]^{2+}$  in the presence of air as a collision gas and at a pressure of  $10^{-6}$  mbar. Impurity peaks are indicated by \*.

As a result of collisional activation, significant proton transfer occurs to give the product ions  $[\text{PbOpropyl}(\text{propan-1-ol})_2]^+$  and  $[\text{PbOpropyl}(\text{propan-1-ol})]^+$ , which also happen to be the dominant ions in the distribution of singly charged complexes shown in Figure 2a. In contrast to previous work with  $[\text{Mg}(\text{ROH})_N]^{2+}$  and  $[\text{Cu}(\text{ROH})_N]^{2+}$ ,<sup>16,20</sup> relative intensities of the proton-transfer products are high as compared with those of the neutral loss peaks, which suggests that we are probing a subtle energy balance between a directly solvated  $\text{Pb}^{2+}$  ion and the solvation of a core of the form  $[\text{Pb}^{2+}\text{OR}^-]$ . As a consequence of Coulombic repulsion between fragments involved in proton transfer, peaks present in a MIKE scan that result from such processes are broad. Therefore, it is impossible to distinguish between protonated versus unprotonated alcohol loss, for example, between  $(\text{propan-1-ol})\text{H}^+$  and  $(\text{propan-1-ol})^+$ . However, it is expected that formation of singly charged lead-propoxide species with a protonated alcohol as a leaving group would be favored. Proton transfer to give  $[\text{PbOpropyl}]^+$  would result in a peak at 4698 eV, which is unfortunately obscured by a large contaminant peak. However, inspection of the base of this peak indicates a significant broadening, which would support the presence of a charge-transfer product in the mass spectrum caused by the loss of  $(\text{propan-1-ol})\text{H}^+$  and four propan-1-ol molecules.

MIKE scans were also performed on CID products from the  $N = 5$  and 4 ions, and in each case the proton-transfer products  $[\text{PbOpropyl}(\text{propan-1-ol})_N]^+$  for  $N = 0, 1,$  and 2 are dominant.

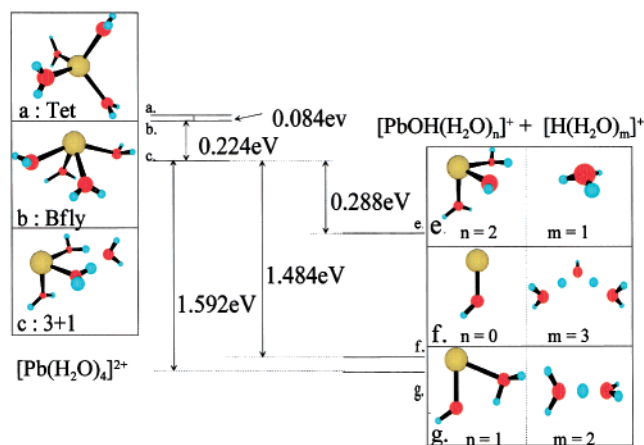


**Figure 3.** Stable structures identified as a result of DFT calculations on the lead/water combination  $[\text{Pb}(\text{H}_2\text{O})_4]^{2+}$ . Structures are labeled as (a) tetrahedral; (b) butterfly; (c) 3 + 1, where three water molecules are bonded directly to the central cation, and a fourth molecule is hydrogen bonded to two of these. Also shown as e, f, and g are possible products of a proton-transfer reaction. Energy differences with respect to the most stable 3 + 1 dication are given in eV, and this aspect of the figure is drawn to scale.

MIKE scans were also used to confirm the identities of  $[\text{Pb}(\text{butan-1-ol})_N]^{2+}$  ions for  $N = 4, 5,$  and 6, and again the results were dominated by proton-transfer processes leading to the formation of  $[\text{PbObutyl}(\text{butan-1-ol})_N]^+$  where  $N = 0, 1,$  and 2. For both propan-1-ol and butan-1-ol, this pattern of behavior correlates with the dominant ions recorded in the mass spectra of the respective singly charged lead/alcohol complexes.

## Discussion

The solvation of lead by this series of hydrogen bonding solvents represents a unique system, where the subtle interplay between a moderate/soft acid ( $\text{Pb}^{2+}$ ) and a progression of bases with different degrees of polarizability (softness) can be examined. A general observation from the experimental work detailed above is that as the length of R, the alkyl chain, increases so does the propensity for ROH to solvate  $\text{Pb}^{2+}$  successfully. Supporting computational work has sought to quantify this behavior and, as a result, produce an interpretation of the factors responsible for the stabilization of  $\text{Pb}^{2+}$  by hydrogen bonding solvents that appears to equate with a HSAB picture of events. The approach has been to consider the relative stability of a given  $[\text{Pb}(\text{ROH})_4]^{2+}$  complex as compared with realistic products from a proton-transfer step, that is,  $[\text{PbOR}(\text{ROH})_{2-x}]^+ + \text{ROH}_2^+(\text{ROH})_x$ . Essentially, there are three main questions posed by the experimental results that the calculations were intended to answer:

(1) For  $R = \text{H}$ , methyl, and ethyl, do the gas-phase structures adopted by the corresponding  $\text{Pb}(\text{II})$  complexes favor proton transfer, and, if so, what form does the protonated product take?

(2) What electronic changes occur on going from  $R = \text{H}$  or  $\text{CH}_3$  to  $R = \text{CH}_3\text{CH}_2\text{CH}_2$  that enable the latter to stabilize  $\text{Pb}(\text{II})$ ?

(3) What can be learned about the Lewis acidity of  $\text{Pb}(\text{II})$ ?

Figure 3 presents results from geometry optimizations performed on  $[\text{Pb}(\text{H}_2\text{O})_4]^{2+}$ . The left-hand side of this figure illustrates various configurations of the  $[\text{Pb}(\text{H}_2\text{O})_4]^{2+}$  ion, and the right-hand side shows a selection of possible proton-transfer products. Energy differences between the most stable  $\text{Pb}(\text{II})$  complex, other trial  $\text{Pb}(\text{II})$  structures, and various proton-transfer

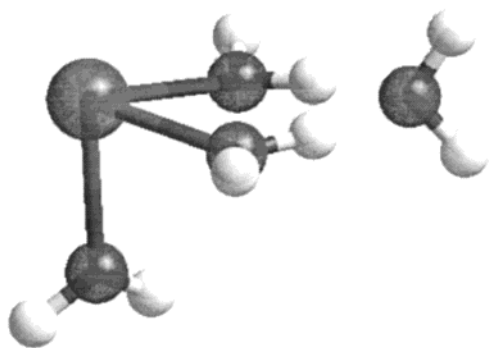


**Figure 4.** Expanded view of the 3 + 1 structure, which from the calculations, is identified as being the most stable  $[\text{Pb}(\text{ROH})_4]^{2+}$  combination for R = H, methyl, ethyl, and 1-propyl.

products are shown. Although concentrating on a single-sized complex, these calculations are considered to illustrate patterns of behavior that may be general to ions covering a range of sizes. For  $[\text{Pb}(\text{H}_2\text{O})_4]^{2+}$ , the lowest energy structure has three water molecules bound directly to the central dication, that is, in a first solvation shell, and an additional water molecule hydrogen bonded in a secondary shell via two (proton) acceptor bonds (denoted as a 3 + 1 structure). Figure 4 presents an expanded view of the 3 + 1 structure, and a frequency analysis confirms this structure as a local minimum on the potential energy surface. The highest energy structure (a) for  $[\text{Pb}(\text{H}_2\text{O})_4]^{2+}$  was obtained when the symmetry of the complex was confined to  $T_d$ . This result is not too surprising in the light of lone pair–ligand repulsion induced by the stereochemically active 6s electrons on the central lead cation.<sup>30</sup> We shall return to a discussion of this point later. The intermediate butterfly-like structure ((b) and denoted b'fly) is best visualized as a distorted square planar structure where all of the ligands are positioned below the horizontal mirror plane. This structure was achieved by restricting the symmetry to  $C_{2v}$  with a tolerance of 0.5 Å during optimization, and under such conditions it represents a local minimum on the potential energy surface. Butterfly-like structures are favored over tetrahedra because of the reduced influence of 6s lone pair repulsion.

In answer to the first part of question 1, it is clear that the 3 + 1 configuration presents the most likely starting structure from which proton transfer can be initiated to yield any of the products listed in Figure 3 (e, f, or g). The ligands in this structure are crowded into approximately one-eighth of the available spherical volume surrounding the central lead cation, and, as a result, increased ligand–ligand repulsion is likely to facilitate the loss of a protonated water molecule (or molecules). As there is no experimental evidence for the complex  $[\text{Pb}(\text{H}_2\text{O})_4]^{2+}$ , and these particular calculations provide no indication of the barrier heights to proton transfer, it is necessary to speculate on a mechanism for this process. If we consider the lowest energy 3 + 1 structure, the oxygen atom of the second sphere water molecule is almost equidistant between the protons of the two first sphere water molecules (O–H<sub>1</sub> 1.58 Å, O–H<sub>2</sub> 1.6 Å). These protons are also further from their respective O atoms (1.03 and 1.02 Å) than the average of 0.99 Å found for the distal coordinated water molecule and the remaining protons in the H-bonded first shell molecules. Using either of the two methods of charge analysis discussed earlier (MPA or NPA), we found that the acceptor protons in the hydrogen bonds carry

**Table 1.** Change in Energy on Going from  $[\text{Pb}(\text{ROH})_4]^{2+}$  in a 3 + 1 Geometry to Each of the Specified Alternative Structures

	tetrahedral <sup>a</sup>	b'fly <sup>a</sup>
H <sub>2</sub> O	29.7	21.6
methanol	50.9	56.1
ethanol	35.6	40.7
propan-1-ol	35.8	35.7

<sup>a</sup> Energies are in kJ mol<sup>-1</sup>.

**Table 2.** Energy Difference on Going from  $[\text{Pb}(\text{ROH})_4]^{2+}$  in a 3 + 1 Geometry to Each of the Specified Charge-Transfer Products  $[\text{PbOR}(\text{ROH})_n]^{+} + (\text{ROH})_m\text{H}^{+}$

	$n = 2, m = 1^a$	$n = 0, m = 3^a$	$n = 1, m = 2^a$
H <sub>2</sub> O	-27.79	-143.18	-153.6
methanol	-83.07	-59.24	-139.32
ethanol	-69.47	-90.12	-141.93
propan-1-ol	-62.81	-86.74	-129.68

<sup>a</sup> Energies are in kJ mol<sup>-1</sup>.

a slightly larger positive charge than is seen on the distal water. In addition, the oxygen atom of the second shell water molecule carries a slightly less negative charge than is found on those molecules in the first shell. Therefore, the physical circumstances would certainly appear to favor proton abstraction of some form by the second shell water molecule.

The calculated stable structural forms identified for other  $[\text{Pb}(\text{ROH})_4]^{2+}$  complexes and their proton-transfer products are similar to those reported in Figure 3 for water. Table 1 lists energy differences between the stable 3 + 1 form of doubly charged structure and the less stable b'fly and  $T_d$  isomers. For methanol and ethanol, the b'fly structure is less stable than the  $T_d$ , and for propanol, the two alternatives are approximately equal in energy with respect to the 3 + 1 form. The results in Table 1 suggest that across the ROH range, the stability of the 3 + 1 structure relative to the  $T_d$  and b'fly structures is greatest for methanol; however, the absolute validity of such a comparison is uncertain given that we are predominantly concerned with relative energies between structures with the same atomic composition.

Table 2 shows the relative ordering of the energies of the proton-transfer products, where it can be seen that two of the three alcohols follow the same pattern seen for water. For water and all three alcohols, the most stable proton-transfer products correspond to the formation of  $[\text{PbOR}(\text{ROH})]^{+} + (\text{ROH})_2\text{H}^{+}$ . Proton transfer to these lowest energy products ( $n = 1, m = 2$ ) is most exothermic for water, and, in general, as the length of the alkyl chain increases, the calculated exothermicity decreases. Although the results show that proton solvation in the form of  $(\text{H}_2\text{O})_2\text{H}^{+}$  or  $(\text{ROH})_2\text{H}^{+}$  as a product would appear to make an important contribution to proton transfer, it does not necessarily drive the process. The order of reaction exothermicity is  $\text{H}_2\text{O} > \text{ROH}$ , but proton affinities follow the order  $\text{ROH} > \text{H}_2\text{O}$ . Clearly, what happens in the other, metal-containing product ion is also significant in determining the outcome of proton transfer.

With regard to the  $[\text{Pb}(\text{ROH})_N]^{2+}$  complexes, the degree of covalency of the bond between the central metal ion and the oxygen donor atoms appears to have implications for stability. Figure 5 shows the results of two separate methods for analyzing charge populations on the lead and oxygen atoms in  $[\text{Pb}(\text{ROH})_4]^{2+}$  complexes. Both MPA and NPA exhibit similar trends regarding

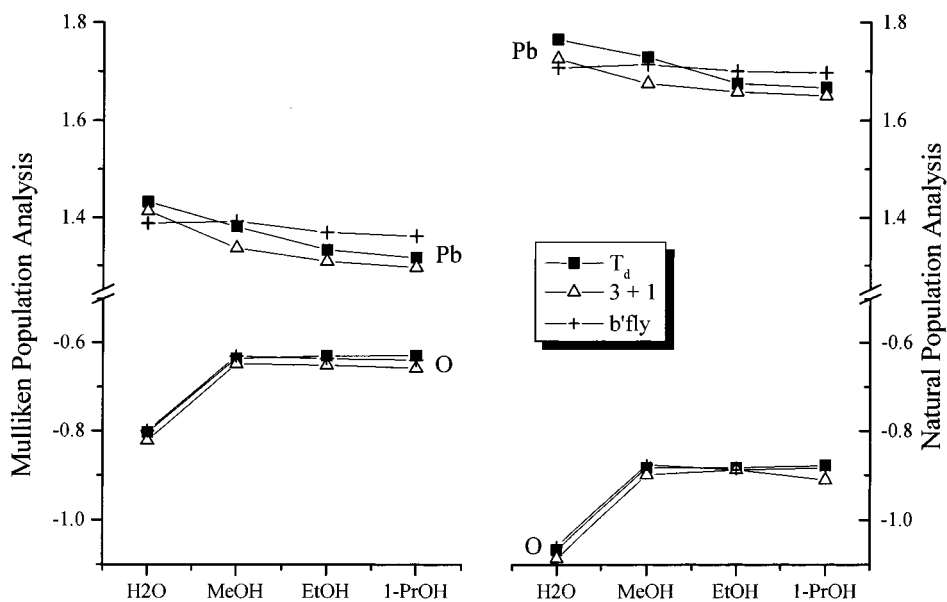


**Figure 5.** Results of a charge population analysis performed on different structural isomers of the  $[Pb(ROH)_4]^{2+}$  cation. Plotted are the charge on the central lead cation and the average charge calculated for oxygen atoms on the donating ligands. For the 3 + 1 structures, only ligands in the first solvation shell are considered. The LHS of the figure gives results from a Mulliken population analysis (MPA) performed using ADF and the RHS results from a natural population analysis (NPA) performed using Gaussian 98.

the variation in charge density as the chain length of the ligand is altered. The charge on the oxygen donor atom has been averaged over four atoms for the  $T_d$  and  $b'$ fly structures, and over the three oxygen atoms directly coordinated to lead for the 3 + 1 structures. To answer question 2 above, it is necessary to consider the changes in ligand behavior that occur through the series of alcohols. As the alkyl chain length increases, the positive charge on the central lead atom decreases, as does the average negative charge on the oxygen donor atoms. In effect, alkyl substitution leads to an increase in polarization of electrons away from the oxygen lone pair and toward the positive charge on the central metal ion. Irrespective of which method is used to analyze electron populations, the calculations show that these polarizing effects are at a maximum when the ligand is propan-1-ol (by implication, this trend should also extend to butan-1-ol). In addition, most examples show that electron polarization is of greatest benefit to Pb(II) when the ligands adopt a 3 + 1 structure. The parent ion intensities given in Figure 2a show  $[Pb(\text{propan-1-ol})_4]^{2+}$  to be the most stable doubly charged complex ion formed with this ligand, and the calculations suggest that stability is because of the depolarizing effect of the 3 + 1 arrangement of ligands on the central lead cation. Increasing the length of the alkyl chain effectively softens the base, which in terms of the HSAB principle should make the corresponding alcohol more receptive to stabilizing a soft Lewis acid, such as Pb(II), which is exactly what is observed in the experiments. This argument serves to answer question 2, as to why solvation of Pb(II) is possible with propan-1-ol and butan-1-ol. In addition to the stronger lead–oxygen bond formed, the bulkiness of these ligands and a weakening of the hydrogen bonds formed in the 3 + 1 structure will lessen the chance of proton transfer in lead(II) complexes containing these alcohols.

These effects are shown in a more quantitative manner with reference to an analysis of orbital population performed using ADF. Table 3 shows results for the doubly charged lead–water and lead–alcohol complexes in terms of orbital occupancy on the central lead atom. The extent of electron donation in the

**Table 3.** MPA and NBO Analysis of Pb(II) for Each Ligand Type in a 3 + 1 Structure

complex	MPA calculation on Pb(II) <sup>a</sup>	NBO analysis of Pb(II) LP occupancy <sup>b</sup>
$[Pb(H_2O)_4]^{2+}, 3 + 1$	6s(1.64) 6p(0.64) sp <sup>0.39</sup>	s(96.48%) p 0.04(3.52%) (1.99211)
$[Pb(MeOH)_4]^{2+}, 3 + 1$	6s(1.60) 6p(0.75) sp <sup>0.47</sup>	s(97.31%) p 0.03(2.69%) (1.98874)
$[Pb(EtOH)_4]^{2+}, 3 + 1$	6s(1.48) 6p(0.82) sp <sup>0.56</sup>	s(97.25%) p 0.03(2.75%) (1.98784)
$[Pb(PrOH)_4]^{2+}, 3 + 1$	6s(1.40) 6p(0.85) sp <sup>0.61</sup>	s(97.13%) p 0.03(2.87%) (1.98637)

<sup>a</sup> Mulliken population analysis of electron donation from each ligand type to Pb(II) (ADF calculation). <sup>b</sup> Natural bond orbital analysis of the lone pair occupancy on Pb(II) (Gaussian 98 calculation).

most stable 3 + 1 structure is listed according to the size of the ligand. In keeping with the results seen in Figure 5, the alternative measure of orbital population, MPA performed under ADF, yields a lower electron density than is found with NPA; however, the qualitative trends are very similar. As the ligand changes from water through to propanol, electron donation into the 6p orbital increases, and, as a result, the overall charge on the lead cation decreases. Of the three “isomers” studied with each ligand, the 3 + 1 structure in each case presents the highest 6p/6s population ratio within each ligand type on moving from the least stable tetrahedral to the most stable 3 + 1 structure. This trend is accompanied by a further increase in the 6p/6s ratio as the ligand involved is softened, that is, on moving from water to propan-1-ol. In an analysis given by Bock et al.,<sup>30</sup> it was concluded that softer ligands exhibit a greater degree of electron transfer toward Pb(II) and that the corresponding increase in p orbital population results in the accompanying metal–ligand bonds becoming more covalent. These same characteristics match the trend seen on moving from water to propan-1-ol as a ligand.

To complement the pattern of electron transfer seen for the Pb(II) complexes, we have also sought to identify any marked

changes the ligands might make to the 6s lone pair resident on the lead cation. Lone pair occupancies have been calculated from a natural bond orbital (NBO) analysis, and these results are also shown in Table 3. For the 3 + 1 complexes, the lone pair is predominantly 6s but is influenced by a small 6p contribution (3.52% with water as a ligand, 2.87% with propan-1-ol). Within each ligand type, the p orbital contribution to the lone pair is greatest for the 3 + 1 isomer, is less marked for the b'fly structure, and is (as expected) almost absent for the  $T_d$  structures. From the analysis given by Bock et al.,<sup>30</sup> enhanced p character in the lone pair appears to be synonymous with hemi-directed hard ligands that form ionic bonds with the metal ion. Once again, the trend seen here fits a pattern whereby there is a gradual softening of the ligands as the length of the alkyl chain increases. The level of p character in the 3 + 1 structures for each of the ligands examined suggests that the lone pair is stereochemically active in every case. Because these structures are also found to be lowest in energy, it would appear that the close proximity of ligands in a strongly hemi-directed structure provides a very favorable starting point from which proton transfer to yield a metal hydroxide products may occur. On the evidence presented in Table 3, water should be the most strongly hemi-directed ligand and propanol the least; thus, a contribution to reaction exothermicity in the case of water could take the form of a release in strain energy between neighboring ligands.

Bock et al.<sup>30</sup> used ab initio methods to examine a range of structures associated with divalent lead complexes containing four ligands (including the sequence H<sub>2</sub>O, H<sub>2</sub>S, H<sub>2</sub>Se, H<sub>2</sub>Te). This latter sequence is analogous to that considered here in terms of a gradual softening of the base, and Bock et al.<sup>30</sup> reported trends very similar to those identified here: hard ligands have less electron transfer to lead, exhibit ionic bonding, and the lone pair has p character; soft ligands reverse these trends. Bock et al.<sup>30</sup> did not explore any 3 + 1 structures; however, they did find significant deviations from  $T_d$  symmetry to yield complexes with structures similar to the b'fly isomers reported here. Hemi-directed configurations are prevalent in crystallographic data on Pb(II), and Bock et al.<sup>30</sup> noted the preference for oxygen- (and nitrogen-) containing ligands to form such structures, particularly when present in small numbers.

## Conclusions

Direct solvation of Pb(II) by ligands of the general form ROH is only observed when R ≥ propyl, and a qualitative analysis of this behavior equates stability with a gradual softening of the ROH base to match the acidic character of the lead cation. Although it has not been possible to calculate full reaction potential energy profiles, dft calculations show that several factors contribute to the stability (and instability) of this series of complexes. Charge population analysis reveals that underpinning stability is a requirement for any solvent (ligand) to reduce the ionic character of the Pb(II)–O bond. This criterion extends even to the products of proton transfer, where we note that increased solvation enhances the stability of the hydrolysis product when water is the ligand, but destabilizes the same product for the case of 1-propanol. The hemi-directing nature of the 6s lone pair on Pb(II) appears to facilitate proton transfer by forcing ligands closer together. This stereochemical effect is strongest in water, but is counteracted by bulkier ligands, such as propan-1-ol. Finally, the proton transfer to yield specific

reaction products is significantly more exothermic in the case of water than for propan-1-ol.

We believe these experimental observations to be the first example of a system where it has been possible to fine-tune the physical properties of a base to match a Lewis acid. In this context, it is of interest to compare the gas-phase behavior of Pb(II) with that of Cu(II). As noted earlier, these metals have very similar p*K*<sub>a</sub> values, and within the HSAB principle they are both frequently classified as borderline soft acids. However, Cu(II) readily forms stable [Cu(H<sub>2</sub>O)<sub>*N*</sub>]<sup>2+</sup> complexes which can be isolated down to *N* = 3; in addition, stable complexes have been reported between Cu(II) and several of the alcohols considered here.<sup>16,25</sup> In contrast, we have found many of the corresponding complexes with Pb(II) to be unstable. We believe this fundamental difference in behavior to be related to the nature of the primary solvation unit adopted by each of the metal ions in the gas phase. For data recorded by us on the solvation of Cu(II),<sup>25</sup> Bérces, Ziegler, and co-workers<sup>45</sup> have shown that the ion preferentially coordinates four water molecules in a square planar arrangement. Additional ligands then form a secondary ring which is hydrogen bonded to the primary shell. These charge-enhanced hydrogen bonds are calculated to be stronger than the alternative arrangement, which is in direct coordination to the Cu(II) axial sites. Although the primary square-planar structure is subject to Jahn–Teller distortion,<sup>45</sup> this is not sufficient to destabilize the water molecules. There are two significant differences between these results for [Cu(H<sub>2</sub>O)<sub>*N*</sub>]<sup>2+</sup> complexes and those presented here for [Pb(H<sub>2</sub>O)<sub>4</sub>]<sup>2+</sup>. First, the most stable primary solvation unit calculated for [Pb(H<sub>2</sub>O)<sub>4</sub>]<sup>2+</sup> consists of three water molecules attached to the central metal ion, with the fourth molecule forming a secondary shell bound by hydrogen bonds. The position of this latter water molecule would provide a natural starting point for the formation of a salt bridge, which calculations suggest should facilitate proton transfer.<sup>46</sup> Such reactions have previously been identified in experiments on small [Mg·(H<sub>2</sub>O)<sub>*N*</sub>]<sup>2+</sup> clusters.<sup>47</sup> A second important consideration is the fact that the three molecules located on Pb(II) are strongly influenced by the presence of a stereochemically active lone pair of electrons, which may occupy significantly more coordination space than does a single ligand bond. For Pb(II), we conclude that three primary shell water molecules are not sufficient to stabilize the ion and that subsequent hydrolysis is aided by both hydrogen bonding and steric interactions induced by the lone pair electrons on the metal ion. In contrast, four primary-shell water molecules in a square-planar arrangement are sufficient to stabilize Cu(II) against hydrolysis even in the presence of additional hydrogen bond formation.

**Acknowledgment.** The authors would like to thank EPSRC for financial assistance with the experimental program, for the award of studentships to G.A.-B., B.D., and L.P., and for the award of an Advanced Research Fellowship to H.C. All calculations were performed on an ONYX 2 belonging to the Sussex High Performance Computing Initiative.

JA011261R

(45) Bérces, A.; Nukada, T.; Margl, P.; Ziegler, T. *J. Phys. Chem. A* **1999**, *103*, 9693.

(46) Beyer, M.; Williams, E. R.; Bondybey, V. E. *J. Am. Chem. Soc.* **1999**, *121*, 1565.

(47) Barran, P. E.; Walker, N. R.; Stace, A. J. *J. Chem. Phys.* **2000**, *112*, 6173.